permanent wavelike deformation only occured on the outer surface of these MWCNTs. We speculate that when the outer layer of the MWCNT breaks at these large stresses, the accumulated elastic energy is released and generates a stress wave; the stress wave travels through the outer surface of the MWCNT and permanently deforms it (*31*). A second possibility is that an accordia-like relaxation of the outer shell onto the inner section occurred immediately after the breaking of the outer shell. Ribbon-like structures were also often seen in the TEM images of the MWCNT fragments (Fig. 4C) and might result in the section of the outer shell from which the inner section has been pulled out. Radial collapse of the MWCNT fragment (Fig. 4D) was also seen. At high tensile strain, the MWCNT experiences a Poisson contraction, which could trigger radial collapse. Partial, and total, radial collapse of MWCNTs has been previously reported (*16*, *32*, *33*). Observation of these types of fragments suggests that the effect of large tensile load and of fracture on nanotube structure will be a fascinating area for further study. Future directions include attempting mechanical-loading measurements on SWCNT ropes and individual SWCNTs, as well as on other types of nanotubes such as boron nitride, and studying the influence of strain rate, temperature, and chemical environment.

References and Notes

1. B. I. Yakobson, in *Fullerenes—Recent Advances in the Chemistry and Physics of Fullerenes and Related Materials*, R. S. Ruoff and K. M. Kadish, Eds. (Electrochemical Society, Pennington, NJ, 1997), vol. 5 (97–42), pp. 549–560.
2. ———, M. P. Campbell, C. J. Brabec, J. Bernholc, *Comput. Mater. Sci.* **8**, 341 (1997). The strain rate in this computer simulation was extremely high.
3. B. T. Kelly, *Physics of Graphite* (Applied Science, London, 1981).
4. B. I. Yakobson, C. J. Brabec, J. Bernholc, *Phys. Rev. Lett.* **76**, 2511 (1996).
5. J. P. Lu, *J. Phys. Chem. Solids* **58**, 1679 (1997).
6. R. S. Ruoff and D. C. Lorents, *Carbon* **33**, 925 (1995).
7. B. I. Yakobson, *Appl. Phys. Lett.* **72**, 918 (1998).
8. P. Zhang, P. E. Lammert, V. H. Crespi, *Phys. Rev. Lett.* **81**, 5346 (1998).
9. M. Buongiorno Nardelli, B. I. Yakobson, J. Berhholc, *Phys. Rev. B* **57**, R4277 (1998).
10. ———, *Phys. Rev. Lett.* **81**, 4656 (1998).
11. P. Poncharal, Z. L. Wang, D. Ugarte, W. A. de Heer, *Science* **283**, 1513 (1999).
12. A. Krishnan, E. Dujardin, T. W. Ebbesen, P. N. Yianilos, M. M. J. Treacy, *Phys. Rev. B Condens. Matter Mater. Phys.* **58**, 14031 (1998).
13. E. W. Wong, P. E. Sheehan, C. M. Lieber, *Science* **277**, 1971 (1997).
14. J.-P. Salvetat *et al.*, *Adv. Mater. (Weinheim, Ger.)* **11**, 161 (1999).
15. D. A. Walters *et al.*, *Appl. Phys. Lett.* **74**, 3803 (1999).
16. M. F. Yu, T. Kowalewski, M. J. Dyer, R. S. Ruoff, in preparation.
17. O. Lourie, D. M. Cox, H. D. Wagner, *Phys. Rev. Lett.* **81**, 1638 (1998).
18. H. D. Wagner, O. Lourie, Y. Feldman, R. Tenne, *Appl. Phys. Lett.* **72**, 188 (1998).
19. A. P. Levitt, *Whisker Technology* (Wiley-Interscience, New York, 1970).
20. M. F. Yu *et al.*, *Nanotechnology* **10**, 244 (1999).
21. Experimental details are available at *Science* Online at www.sciencemag.org/feature/data/1046083.shl.
22. The SEM nanostressing stage mainly consists of two parts. One is an *x-y* sliding stage driven by two linear picomotors, with a quadrant piezotube on top; another is a *z* stage driven by a linear picomotor, with a theta stage driven by a rotating picomotor on top. The linear picomotor has a step size of about 30 nm, and the rotating picomotor has a step resolution of better than 0.1 mrad. The stage can travel 6 mm in three dimensions and rotates continuously in the θ direction along the *x* axis. All picomotors were driven with a control pad that can manually set constant velocities for the extension and retraction of the picomotor driving shaft. The piezotube can give subnanometer resolution in three axes with several microns of travel range. Operation of the stage inside the SEM showed smooth travel and no interference with the SEM imaging. The LEO 982 FE-SEM has a stated resolution of 1 nm at an operating voltage of 30 kV. The SEM chamber vacuum was better than 3×10^{-6} torr with the stage inside. The typical tensile-loading experiment lasts 1 min, and the typical tensile-loading strain rate is about 0.3 s^{-1}, according to the recorded video tape.
23. There are three soft cantilevers in series on the same side of the AFM probe. The nominal lengths *L* of these three separate silicon spring-beam type cantilevers (the cs12 contact mode AFM probe was supplied by NT-MDT) are 350, 300, and 250 μm; all have a nominal width, *w*, of 35 μm and a nominal thickness, *t*, of 1 μm. The force constant (*K*) of each can be calculated with the formula $K = Ewt^3/4L^3$. (Here *E* is for a silicon single crystal, 145 GPa.) We measured *L*, *w*, and *t* in an SEM and used the measured, not the nominal, values to calculate *K*.
24. T. Fujii *et al.*, *J. Vac. Sci. Technol. B* **9**, 666 (1991).
25. H. W. P. Koops *et al.*, *Jpn. J. Appl. Phys. Part 1* **33**, 7099 (1994).
26. G. G. Tibbetts and C. P. Beetz, *J. Phys. D Appl. Phys.* **20**, 292 (1987).
27. If we use the surface energy (γ) of graphite (~0.24 J m^{-2}) and the OD of this MWCNT (33 nm), the capillary force between MWCNT layers, which is equal to $2\pi OD\gamma$, is calculated to be ~50 nN; also, with use of the shear strength of graphite (~0.48 MPa) and the initial contact length between MWCNT layers (~10 mm), the shear force needed for sliding between nested layers would be ~50 nN. Because each of these values exceeds the measured upper limit force, further study of the energetics and forces involved in pullout is needed.
28. R. Bacon, *J. Appl. Phys.* **31**, 283 (1959).
29. D. E. Soule and C. W. Nezbeda, *J. Appl. Phys.* **39**, 5122 (1968).
30. M. S. Dresselhaus, G. Dresselhaus, K. Sugihara, I. L. Spain, H. A. Goldberg, *Graphite Fibers and Filaments*, Springer Series in Materials Science (Springer-Verlag, New York, 1988), vol. 5.
31. M. A. Meyers, *Dynamic Behavior of Materials* (Wiley, New York, 1994).
32. R. S. Ruoff, J. Tersoff, D. C. Lorents, S. Subramoney, B. Chan, *Nature* **364**, 514 (1993).
33. N. G. Chopra *et al.*, *Nature* **377**, 135 (1995).

34. This work was partially supported by the Office of Naval Research and the Defense Advanced Research Projects Agency under Navy grant N000014-99-1-0769, by NSF under the New Tools and Methods for Nanotechnology grant NSF-DMR 9871874, and by Zyvex. We thank R. E. Smalley's group at Rice University for the MWCNT samples and the staff at the Materials Science Center at the University of Wisconsin (UW) for their assistance (the NSF Materials Research Science and Engineering at UW provides support for the UW electron microscope facilities). We appreciate use of the Washington University TEM facility overseen by P. Gibbons; and we thank B. Files, T. Kowalewski, B. Yakobson, and R. Carpick for commenting on the manuscript. R.S.R. would like to dedicate this paper to the memory of Herbert S. Gutowsky.

7 October 1999; accepted 2 December 1999

Cloning and Heterologous Expression of the Epothilone Gene Cluster

Li Tang, Sanjay Shah, Loleta Chung, John Carney, Leonard Katz, Chaitan Khosla, Bryan Julien*

The polyketide epothilone is a potential anticancer agent that stabilizes microtubules in a similar manner to Taxol. The gene cluster responsible for epothilone biosynthesis in the myxobacterium *Sorangium cellulosum* was cloned and completely sequenced. It encodes six multifunctional proteins composed of a loading module, one nonribosomal peptide synthetase module, eight polyketide synthase modules, and a P450 epoxidase that converts desoxyepothilone into epothilone. Concomitant expression of these genes in the actinomycete *Streptomyces coelicolor* produced epothilones A and B. *Streptomyces coelicolor* is more amenable to strain improvement and grows about 10-fold as rapidly as the natural producer, so this heterologous expression system portends a plentiful supply of this important agent.

The epothilone polyketides (*1*) stabilize microtubules by means of the same mechanism of action as the anticancer agent Taxol (*2*). However, epothilones are advantageous in that they are effective against Taxol-resistant tumors and are sufficiently water soluble that they do not require deleterious solubilizing additives (*3*). For these reasons, epothilone is widely perceived as a potential successor to Taxol (*4*).

The paucity of epothilones currently obtainable represents a major impediment to clinical evaluation of this important agent. The epothilone producer *Sorangium cellulosum* yields only about 20 mg $liter^{-1}$ of the polyketides and has a 16-hour doubling time that makes produc-

KOSAN Biosciences, 3832 Bay Center Place, Hayward, CA 94545, USA.

*To whom correspondence should be addressed. E-mail: julien@kosan.com

tion in this organism economically impractical (*1*). Further, while epothilones A (**1**) and B (**2**) are the most abundant congeners (produced in a 2:1 ratio) in fermentation extracts, 12,13-desoxyepothilone B (**4**; epothilone D) has the highest therapeutic index but is produced in only trace amounts (*4*). Owing to the lack of a satisfactory fermentation process, the total synthesis of epothilones has been pursued as a source of material and in order to develop structure-activity relations (*3*, *5*, *6*). The Danishefsky (*3*, *5*) and Nicolaou (*6*) research groups have reported tour de force efforts for the complete synthesis of epothilone and numerous analogs. However, given the complexity of the over 20 synthetic-step processes, fermentation-based methods are likely to reign as preferred practical approaches for large-scale production of the epothilones.

Here we demonstrate the production of epothilones A and B in a "fermentation-friendly" heterologous host. To accomplish this, we cloned and sequenced the entire 56-kb epothilone gene cluster, which encodes a polyketide synthase (PKS), including a nonribosomal peptide synthetase module, and a cytochrome P450 epoxidase. Introduction of all the genes of the cluster into *Streptomyces coelicolor* CH999 led to the production of epothilones A and B. Heterologous production of the cytochrome P450 EpoK in *Escherichia coli* and an in vitro assay provided direct evidence that this enzyme catalyzes the conversion of desoxyepothilone (**3** and **4**) into epothilone (**1** and **2**) as the final step in epothilone biosynthesis.

Type I PKSs and nonribosomal peptide synthetases (NRPSs) are large multifunctional protein complexes organized in a modular fashion. Each PKS module activates and incorporates a two-carbon (ketide) unit building block into the polyketide backbone. The number and order of modules, and the types of ketide-modifying enzymes within each module, determine the structural variations of the resulting products. The epothilones show two interesting structural variations when compared to a prototypical polyketide such as 6-deoxyerythronolide B: a thiazole moiety and a geminal dimethyl group. A gene cluster that includes a NRPS module flanked by PKS modules, one of which contains an embedded methyl transferase, could produce such variations.

Using polymerase chain reaction (PCR)–generated hybridization probes (*7*), we isolated four overlapping cosmid clones from a genomic library of *S. cellulosum* strain SMP44. DNA sequence analysis revealed eight open reading frames (ORFs) that span over 56 kb (Fig. 1). They include *epoA* (encoding the 149-kD loading domain), *epoB* (158 kD, a NRPS module), *epoC* (193 kD, PKS module 2), *epoD* (765 kD, PKS modules 3 to 6), *epoE* (405 kD, PKS modules 7 and 8), *epoF* (257 kD, PKS module 9 plus a thioesterase domain), *epoK* (47 kD, a cytochrome P450), and an ORF immediately downstream of *epoK* that encodes a protein with three membrane-spanning regions (ORF1).

The domain organization of the epothilone gene cluster is consistent with the structure of epothilone. The role of the enoylreductase (ER) domain within the loading module is unknown; it may be cryptic or it may play a role in the oxidation of the thiazoline to the thiazole. The only function absent is a dehydratase (DH) domain in module 4, which would generate a cis double bond between carbons 12 and 13. Dehydration could occur either in the next module (which possesses an active DH domain) by an atypical process, or by action of a post-PKS modifying enzyme. Another intriguing feature of the PKS is that the acyltransferase (AT) domain of module 4 accepts either malonyl or methylmalonyl extender units. This relaxed specificity is consistent with the PKS producing both epothilones A and B in the absence of an identifiable separate methyltransferase. A methyltransferase (MT) domain is integrated into module 8 between the DH and ketoreductase (KR) domains and is believed to methylate C-4 of the epothilones to generate the gem-dimethyl function. Similar MT domains have been observed in the PKSs for lovastatin, fumonisin, and yersiniabactin biosynthesis (*8*). Another notable feature of the epothilone polyketide megasynthase is the presence of an NRPS module flanked by two PKS modules. This NRPS module contains signature sequences for recognizing cysteine as well as a cyclization domain, which leads to the formation of the thiazole (*9*).

For heterologous expression of the epothilone gene cluster, and production of epothilone, we used the well-characterized actinomycete *S. coelicolor*. In contrast to *S. cellulosum*, *S. coelicolor* is well understood genetically and genomically and has a doubling time of only 2 hours. Vector systems for the expression of PKS gene clusters in this organism have been described (*10*) and used to synthesize a variety of bacterial and fungal natural products (*11*). The large epothilone biosynthetic gene cluster was cloned into two compatible plasmids (*12*). The *epoA*, *epoB*, *epoC*, and *epoD* genes were cloned as an operon behind the *actI* promoter on a thiostrepton-resistant SCP2* derivative (*13*), whereas *epoE*, *epoF*, *epoK*, and ORF1 were fused as a second operon to the *actI* promoter on an apramycin-resistant pSET152 derivative (*14*). The plasmids were introduced into *S. coelicolor* CH999 (*15*), and transfor-

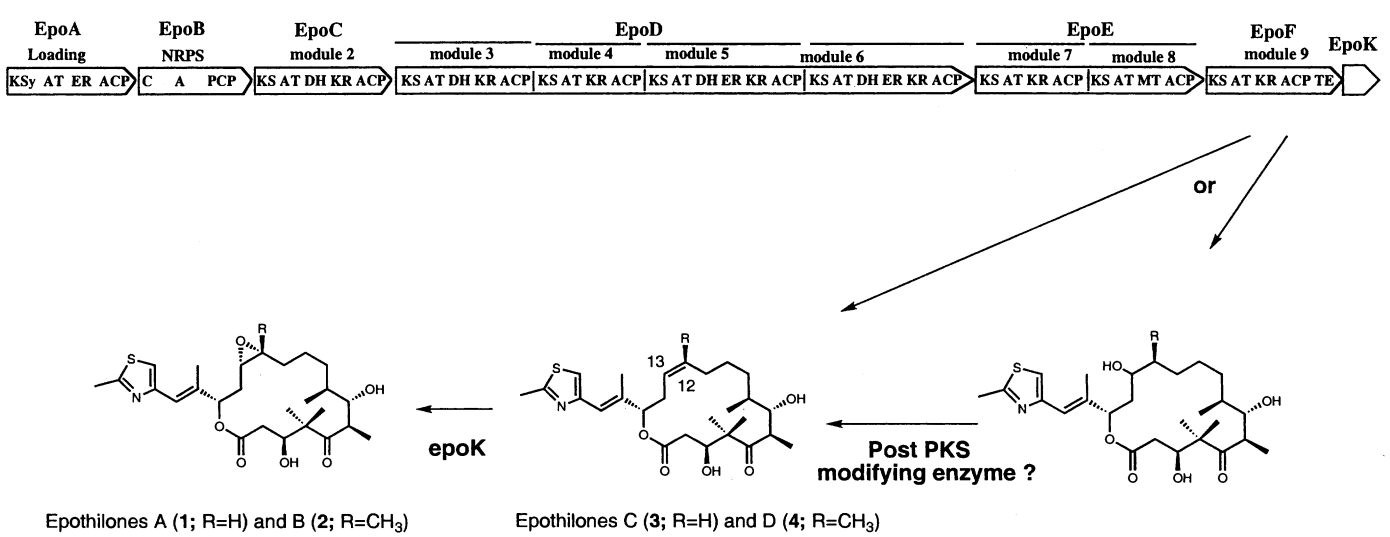

Fig. 1. Modular organization of the epothilone polyketide synthase (PKS). Functional domains of each of the epothilone PKS modules are shown. Stepwise synthesis of epothilones begins at EpoA and ends with the cyclization by the TE domain in EpoF to yield either epothilones C and D or the hypothetical molecule containing the OH group at C-13. Abreviations: KS, β-ketoacyl ACP synthase; KSy, β-ketoacyl ACP synthase containing a tyrosine substitition of the active-site cysteine; AT, acyltransferase; DH, dehydratase; ER, enoylreductase; KR, ketoreductase; MT methyltransferase; ACP, acyl carrier protein; TE, thioesterase; C, condensation; A, adenylation; PCP, peptidyl carrier protein.

mants were grown on R2YE medium. The transformants produced epothilones A and B, as verified by high-performance liquid chromatography (HPLC), mass spectroscopy (MS) of the molecular ions, and, for epothilone A, mass fragmentation pattern (*16*). Recently, deletion of *epoK* and the downstream gene (ORF1) produced epothilones C and D (*17*). Initial yields of the epothilones in these studies were 50 to 100 μg liter^{-1}. Given the high growth rate and pliability of *S. coelicolor* to genetic and conventional strain improvement, this system promises to evolve into the preferred producer of epothilone.

In addition, *epoK* gene was expressed in *E. coli*. EpoK was purified (*18*) and shown to have an ultraviolet (UV)–visible spectrum characteristic of a cytochrome P450 enzyme. The purified protein converted desoxyepothilone B (**4**) to epothilone B (**2**) (*19*), indicating that the epoxidation reaction is the last step in the biosynthetic pathway.

The production of epothilones A and B in *S. coelicolor* demonstrates that the polypeptides encoded by the *epoA-F* and *epoK* genes, and the small molecule precursors in the heterologous host are sufficient for epothilone biosynthesis. The availability of a heterologous expression system portends rapid advancement in several important areas. First, protein and metabolic engineering of the expression system are now possible that, together with conventional strain improvement approaches, will enhance productivity and increase availability of the epothilones. Compared to the poorly understood and slow-growing *S. cellulosum*, *S. coelicolor* offers major advantages, because it is readily amenable to genetic manipulation and replicates about 10-fold faster. Second, it should now be possible to construct an expression system for the currently most attractive clinical candidate, desoxyepothilone, as the sole fermentation product. This could be achieved by two relatively simple modifications that have precedent in the manipulation of PKS gene clusters (*20*): (i) substitution of the nonspecific AT of module 4 with a methylmalonyl-specific AT to prevent formation of epothilones A and C, and (ii) inactivation or omission of *epoK* to prevent conversion of desoxyepothilone to epothilone B. Finally, as demonstrated for erythromycin (*21*), the availability of cloned genes and a plasmid-borne expression system will allow facile manipulation of the epothilone PKS to produce potentially superior epothilone analogs.

References and Notes

1. K. Gerth, N. Bedorf, G. Höfle, H. Irschik, H. Reichenbach, *J. Antibiot.* **49**, 560 (1996).
2. D. M. Bollag *et al.*, *Cancer Res.* **55**, 2325 (1995).
3. D.-S. Su *et al.*, *Angew. Chem. Int. Ed. Engl.* **36**, 2093 (1997).
4. T.-C. Chou *et al.*, *Proc. Natl. Acad. Sci. U.S.A.* **95**, 9642 (1998); T.-C. Chou *et al.*, *Proc. Natl. Acad. Sci. U.S.A.* **95**, 15798 (1998).
5. A. Balog *et al.*, *Angew. Chem. Int. Ed. Engl.* **35**, 2801 (1997).
6. Z. Yang, Y. He, D. Vourloumis, H. Vallberg, K. C. Nicolaou, *Angew. Chem. Int. Ed. Engl.* **35**, 2399 (1995); K. C. Nicolaou *et al.*, *Angew. Chem. Int. Ed. Engl.* **36**, 2097 (1997).
7. Degenerate KS primers were based on soraphen and erythromycin KS sequences with bias to codon usage for the soraphen KS: 5′-CTSGTSKCSSTBCACTSGCSTGC and 5′-TGAYRTGSGCGTTSGTSCCGSWGA. The ~750–base pair PCR product amplified from SMP44 genomic DNA was ligated into pUC118. Six unique KS fragments were used as probes to screen a cosmid library.
8. J. Kennedy *et al.*, *Science* **284**, 1368 (1999); A. M. Gehring *et al.*, *Chem. Biol.* **5**, 573 (1998); L. Hendrickson *et al.*, *Chem. Biol.* **6**, 429 (1999); R. H. Proctor, A. E. Desjardins, R. D. Plattner, T. M. Hohn, *Fungal Genet. Biol.* **27**, 100 (1999).
9. D. Konz and M. A. Marahiel, *Chem. Biol.* **6**, R39 (1999); T. Stachelhaus, H. D. Mootz, M. A. Marahiel, *Chem. Biol.* **6**, 493 (1999).
10. C. M. Kao, L. Katz, C. Khosla, *Science* **265**, 509 (1994).
11. R. McDaniel, S. Ebert-Khosla, D.A. Hopwood, C. Khosla, *Science* **262**, 1546 (1993); H. Fu, S. Ebert-Khosla, D. A. Hopwood, C. Khosla, *J. Am. Chem. Soc.* **116**, 4166 (1994); D. J. Bedford, E. Schweizer, D. A. Hopwood, C. Khosla, *J. Bacteriol.* **177**, 4544 (1995); T.-W. Yu *et al.*, *J. Am. Chem. Soc.* **120**, 7749 (1998).
12. Coexpression of the three DEBS genes from multiplasmids produced active PKS in *Streptomyces* [Q. Xue, G. Ashley, C. R. Hutchinson, D. V. Santi, *Proc. Natl. Acad. Sci. U.S.A.* **96**, 11740 (1999)].
13. Plasmid pKOS039-124R was constructed from an intermediate plasmid pKOS039-124 that contained an eryKS5 linker sequence at the 5′ end of the *epoA* gene-coding sequence. The eryKS5 linker coding sequences were cloned as an ~0.4-kb Pac I–Bgl II restriction fragment from plasmid pKOS10-153 into pKOS039-98 to construct plasmid pKOS039-117. The coding sequences for the eryKS5 linker were linked to those for the epothilone loading domain by inserting the ~8.7-kb Eco RI–Xba I restriction fragment from cosmid pKOS35-70.1A2 into Eco RI–Xba I–digested plasmid pLitmus28. The ~3.4-kb Bsa BI–Not I and ~3.7-kb Not I–Hind III restriction fragments from the resulting plasmid were inserted into Bsa BI–Hind III–digested plasmid pKOS039-117 to construct plasmid pKOS039-120. The ~7-kb Pac I–Xba I restriction fragment of plasmid pKOS039-120 was inserted into plasmid pKAO18′ to construct plasmid pKOS039-123. Plasmid pKOS039-124 vector was constructed by ligating the ~34-kb Xba I–Avr II restriction fragment of cosmid pKOS35-70.1A2 with the ~21.1-kb Avr II–Xba I restriction fragment of pKOS039-123. The eryKS5 linker sequences were then replaced by *epoA* gene-coding sequences. To amplify by PCR coding sequences from the *epoA* gene-coding sequence, two oligonucleotides primers were used: N39-73, 5′-GCTTAATTAAGGAGGACACATATGCCCGTCGTGGCGGATCGTCC-3′; and N39-74, 5′-GCGGATCCTCGAATCACCGCCAATATC-3′. The template DNA was derived from cosmid pKOS35-70.8A3. The ~0.8-kb PCR product was digested with restriction enzymes Pac I and Bam HI and then ligated with the ~2.4-kb Bam HI–Not I and the ~6.4-kb Pac I–Not I restriction fragments of plasmid pKOS039-120 to construct plasmid pKOS039-136. Then, the ~5 kb Pac I–Avr II restriction fragment of plasmid pKOS039-136 was ligated with the ~50 kb Pac I–Avr II restriction fragment of plasmid pKOS039-124 to construct the expression plasmid pKOS039-124R.
14. Plasmid pKOS039-126R was constructed from intermediate plasmid pKOS039-126 that contained an eryKS5 linker sequence at the 5′ end of the *epoE* gene-coding sequence. The coding sequences for module 7 were linked from cosmids pKOS35-70.4 and pKOS35-79.85 by cloning the ~6.9-kb Bgl II–Not I restriction fragment of pKOS35-70.4 and the ~5.9-kb Not I–Hind III restriction fragment of pKOS35-79.85 into Bgl II–Hind III–digested plasmid pLitmus28 to construct plasmid pKOS039-119. The ~12-kb Nde I–Nhe I restriction fragment of cosmid pKOS35-79.85 was cloned into Nde I–Xba I–digested plasmid pKOS039-119 to construct plasmid pKOS039-122. To fuse the eryKS5 linker coding sequences with the coding sequences for module 7, the ~1-kb Bsa BI–Bgl II restriction fragment derived from cosmid pKOS35-70.4 was cloned into Bsa BI–Bcl I–digested plasmid pKOS039-117 to construct plasmid pKOS039-121. The ~21.5-kb Avr II restriction fragment from plasmid pKOS039-122 was cloned into Avr II–Xba I–digested plasmid pKOS039-121 to construct plasmid pKOS039-125. The ~21.8-kb Pac I–Eco RI restriction fragment of plasmid pKOS039-125 was ligated with the ~9-kb Pac I–Eco RI restriction fragment of plasmid pKOS039-44 to construct pKOS039-126. The eryKS5 sequences were then replaced by *epoE* sequences as follows. To amplify by PCR sequences from the *epoE* gene–coding sequence, two oligonucleotide primers were used: N39-67A, 5′-GCTTAATTAAGGAGGACACATATGACCGACCGAGAAGGCCAGCTC-CTGGA-3′; and N39-68, 5′-GGACCTAGGCGGGATGCCGGCGTCT-3′. The template DNA was derived from cosmid pKOS35-70.1A2. The ~0.4-kb amplification product was digested with restriction enzymes Pac I and Avr II and ligated with the ~29.5-kb Pac I–Avr II restriction fragment of plasmid pKOS039-126 to construct plasmid pKOS039-126R.
15. D. A. Hopwood *et al.*, *Genetic Manipulation of* Streptomyces*: A Laboratory Manual* (John Innes Foundation, Norwich, UK, 1985).
16. The ethyl acetate extract residues from cultures were fractionated over ODS SPE cartridges [MeCN-H_2O (1:1), followed by MeCN]. The MeCN eluents were analyzed by HPLC–MS on a PE Sciex API100LC MS equipped with an atmospheric pressure chemical ionization source. Ring and orifice voltages were set to 75 and 300 V, respectively, and a dual range mass scan from *m/z* (mass-to-charge ratio) 290 to 330 and 450 to 550 with 0.1 atomic mass unit (amu) resolution was used. HPLC conditions: Metachem 5 μ ODS-3 Inertsil (4.6 mm by 150 mm); H_2O for 1 min, then MeCN for 10 min at 1 ml/min. Epothilone A eluted at 10.2 min under these conditions and gave characteristic ions at *m/z* 494.4 (M+H), 476.4 (M+H-H_2O), 318.3, and 306.4. Epothilone B eluted at 10.5 min and displayed a molecular ion at *m/z* 508.4 (M+H). Authentic samples of epothilone A and B derived from *S. cellulosum* SMP44 were used as reference compounds.
17. L. Tang *et al.*, unpublished results.
18. The pET22b-derived plasmids encoding EpoK fused at either end with His_6 were constructed by PCR. Soluble EpoK was obtained in BL21 (DE3) harboring pREP4-groELS encoding GroEL and GroES [P. Caspers, M. Stieger, P. Burn, *Cell Mol. Biol.* **40**, 635 (1994)]. Purification was performed on a Ni–nitrilotriacetic acid His·Bind resin as recommended (Novagen).
19. The assay was done as described [M. C. Betlach, J. T. Kealey, M. C. Betlach, G. W. Ashley, R. McDaniel, *Biochem.* **37**, 14937 (1998)]. About 1.5 μM NH_2- or COOH-terminal His-tagged EpoK converted 100 μM desoxyepothilone B (**4**) to epothilone B (**2**), in 80 and 60% yields, in 1 hour, respectively. HPLC conditions: Metachem 5 μ ODS-3 Inertsil (4.6 mm by 150 mm); 80% H_2O for 1 min, then 100% MeCN for 10 min at 1 ml/min, with UV (λ_{max} = 250 nm), evaporative light scattering detector and MS detection. Epothilone D eluted at 11.6 min and epothilone B at 9.3 min. The liquid chromatography–MS spectra were obtained by using an atmospheric pressure chemical ionization source with orifice and ring voltages set at 20 and 250 V, respectively, at a mass resolution of 1 amu. Under these conditions, epothilone D shows an [M+H] at *m/z* 493, with observed fragments at 405 and 304; epothilone B shows an [M+H] at *m/z* 509, with observed fragments at 491 and 320.
20. R. McDaniel *et al.*, *Proc. Natl. Acad. Sci. U.S.A.* **96**, 1846 (1999).
21. Q. Xue, G. Ashley, C. R. Hutchinson, D. V. Santi, *Proc. Natl. Acad. Sci. U.S.A.* **96**, 11740 (1999).

22. We are grateful to S. Danishefsky for providing desoxyepothilone B used in the EpoK assay. We thank M. Betlach and G. Ashley for suggestions, H. Tsuruta and R. Goldman for technical assistance, and T. Omba for encouragement. Partially funded by Small Business Innovative Research grant 1 R43 CA79228-01. The epothilone gene cluster sequence has been deposited in GenBank with the accession number AF217189.

18 November 1999; accepted 17 December 1999